

# Experimental Evaluations of the Dual-Excitation Permanent Magnet Vernier Machine

Akio Toba\*, Hiroshi Ohsawa\*, Yoshihiro Suzuki\*\*, Tukasa Miura\*\*, and Thomas A. Lipo\*\*\*

Fuji Electric Co. R&D, Ltd. \*  
1 Fuji-machi, Hino  
Tokyo 191-8502, JAPAN  
Tel: +81-42-586-1102, Fax: +81-42-586-9665  
e-mail: toba-akio@fujielectric.co.jp

Fuji Electric Motor Co. \*\*

The University of Wisconsin - Madison \*\*\*

## Abstract

This paper presents experimental evaluations of the Dual-Excitation Permanent Magnet Vernier Machine, a high torque at low speed motor which has been proposed by the authors. Through the experiments, it is verified that the rated torque of the prototype is 15.1Nm with the stator of 130mm-diameter and 60mm-axial length, which is about 1.5 times higher than the conventional permanent magnet machines of the same size. Cogging torque and torque ripple are confirmed to be very low. The experimental results agreed well with the design and analysis, except that the mechanical and iron losses become higher than expected.

**Key words:** High-torque, Vernier Machine, Permanent Magnet

## 1 Introduction

A Permanent Magnet Vernier Machine (PMVM) has the feature of high torque at low speed, and is thus suitable for direct drive applications [1]-[5]. The high torque at low speed feature is based on the so-called 'magnetic gearing effect,' which is also made use of in most of the stepper motors.

Authors have developed a new type of the PMVM, which was named the Dual-Excitation Permanent Magnet Vernier Machine (DEPMVM)<sup>[5]</sup>, aiming to maximize the torque per volume with a modest value of the inductance. In [5], the authors showed the process of inventing the DEPMVM as well as some of its basic properties obtained from the experiments of a prototype.

This paper presents further details of the experimental evaluations of the prototype DEPMVM. In Section 2, the basis of the proposed DEPMVM is presented, followed by the explanation of the design of the prototype. In Section 3, experimental results of the prototype and discussion with those results are addressed. Conclusions are set forth in Section 4.

## 2 Dual-Excitation Permanent Magnet Vernier Machine

### 2.1 Permanent Magnet Vernier Machine

Fig. 1 shows a half cross-sectional view of a typical PMVM. Its structure is similar to the ordinary surface permanent magnet machines, except that the stator has uniformly pitched teeth on its surface toward the airgap and that the number of the rotor poles is much larger than that of the winding poles. There exists a fundamental rule in the PMVM, which characterizes this machine, requiring

$$Z_2 = Z_1 \pm p \quad (1)$$

where  $p$ ,  $Z_1$ , and  $Z_2$  are the numbers of winding pole-pairs, stator teeth, and rotor pole-pairs, respectively. In the machine in Fig. 1,  $p = 1$ ,  $Z_1 = 18$ , and  $Z_2 = 17$ . This relationship is the key to yield its high torque at low speed characteristics as well as its smooth torque<sup>[1], [4]</sup>. Another remarkable property of the PMVM is that it behaves as a conventional permanent magnet machine from the electric circuit point of view. Therefore, familiar drive strategies like field orientation can be employed.

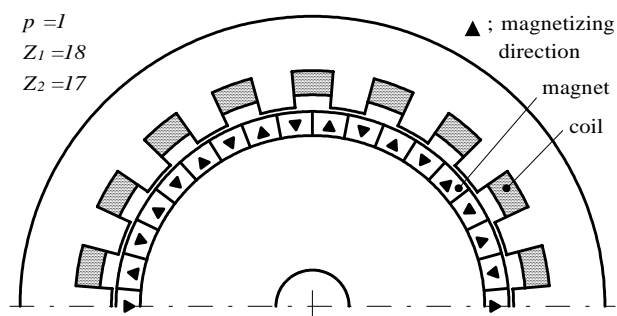


Fig. 1 Permanent Magnet Vernier Machine

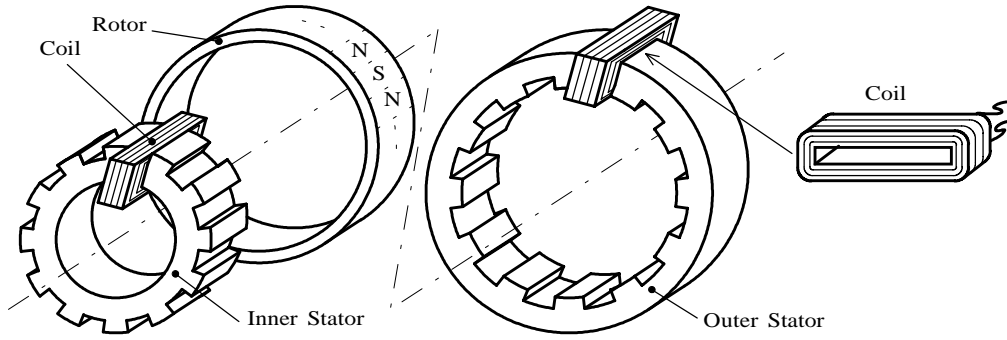


Fig. 2 Structure of the Dual-Excitation Permanent Magnet Vernier Machine

## 2.2 Motivation toward the DEPMVM<sup>[5]</sup>

The key items to improve the characteristics of the PMVM are as follows:

- A small number of the winding poles to obtain higher torque.
- The open slot stator to achieve a high slot fill factor, not the toothed-pole stator.
- Surface-mounted permanent magnet on the rotor to reduce the inductance.
- A larger diameter of the rotor to obtain a larger area of the permanent magnet.

Adopting these factors as well as the solutions of the problems accompanied by the factors, we proposed the Dual-Excitation Permanent Magnet Vernier Machine, DEPMVM, shown in Fig. 2. The main features of the DEPMVM are

- the adoption of the ‘drum’ windings, in which the coils are wound around the stator yoke, and
- a ring shaped rotor with two stators inside and outside of the rotor.

Because of these items, the following merits are brought about.

- The space utilization of the machine becomes very high.
- There is no necessity to fix the coils, which is advantageous with the open slot stator.
- The coil-end becomes shorter than in the conventional winding configuration in many cases.

## 2.3 Prototype machine

A prototype of the DEPMVM has been constructed. Its dimensions are shown in Fig. 3 and its specifications are in Table 1. The prototype has been designed with the aid of the finite element analysis to satisfy the following constraints.

- The outer diameter and the axial length are set to the values shown in Table 1.

- The maximum magnetic flux density in the stator yokes becomes 1.6T when the coil current is 150% of the rated value.
- The permanent magnets are not demagnetized irreversibly with 300% current.

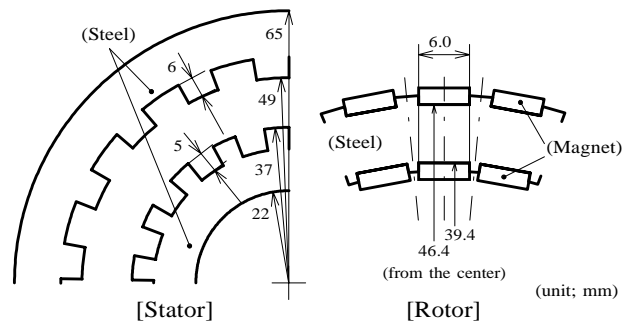


Fig. 3 Major dimensions of the prototype DEPMVM

Table 1 Specifications of the prototype DEPMVM

$Z_1=18, Z_2=17, p=1,$	Slots/pole/phase/stator; 3
	Number of coil turns; 26 (outer), 18 (inner) /slot
	Rated current; 4.4A, Rated speed; 300r/min
	Rated power; 530W, Rated torque; 16.9Nm
	Permanent Magnet; NdFeB( $B_r=1.23T, H_c=-8.9e5$ )
	thickness; 2.0mm
	Steel lamination stack length; 60mm

Fig. 4 shows the pictures of the rotor and the stators. Fig. 5 illustrates the assembly of the prototype machine. There are two bearings on each side of the machine; one is a conventional ball bearing, and the other is a ring-shaped slip bearing which has a relatively high friction. Although the high friction is not desirable, it was chosen this time because of the easiness of the implementation. Several values and parameters with the prototype obtained by the finite element analysis are compared with the experimental results in the next section.



(a) Outer (left) and inner (right) stators with coils



(b) Rotor

Fig. 4 Pictures of the prototype parts

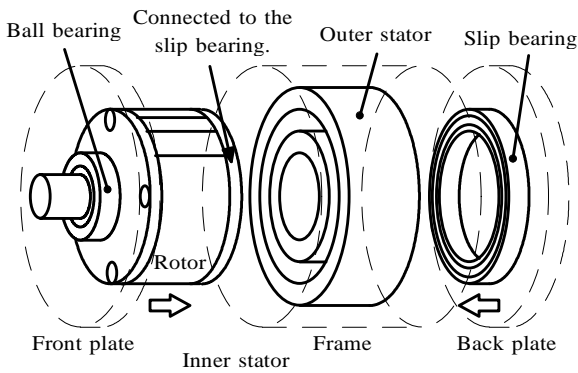


Fig. 5 Assembly of the prototype

### 3 Experimental Evaluations

#### 3.1 Experimental Setups

Two types of tests have been conducted with the prototype; inverter-driven tests (Test A) and generator tests with linear load (Test B). Fig. 6 shows the experimental setups for both of the tests. The prototype machine is connected to a load machine with a mechanical shaft via a torque meter and a position sensor. The load machine is driven by an inverter, which is capable of instantaneous torque control. About the

prototype machine, the fundamental components of the current and the no-load induced voltage of each phase are controlled to be in phase for both of Test A and Test B, which results in the maximum torque per current. In Test A, the sinusoidal PWM inverter to drive the prototype can achieve that condition. In Test B, the capacitors in the load circuit offsets the coil inductance of the prototype machine and then the above-described condition can be realized.

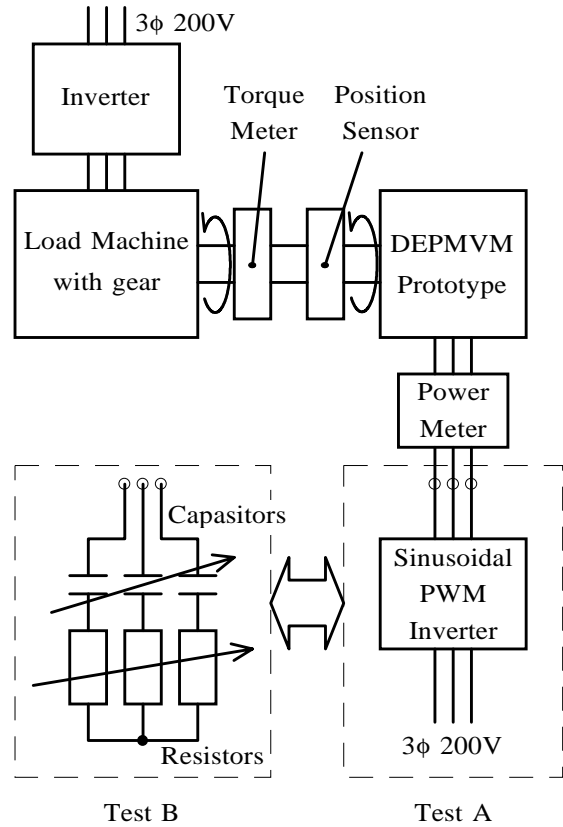


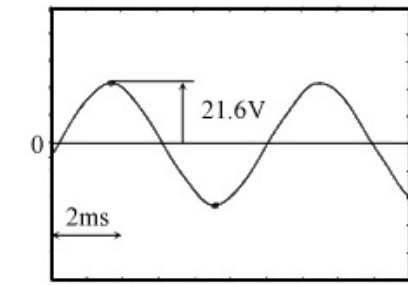
Fig. 6 Schematic of the experimental setups

#### 3.2 Resistance and Inductance

Table 2 indicates the measured and analyzed values of the resistance of one phase coil and the inductance of d- and q-axes. It is noted that good agreements are obtained and that the saliency is negligible.

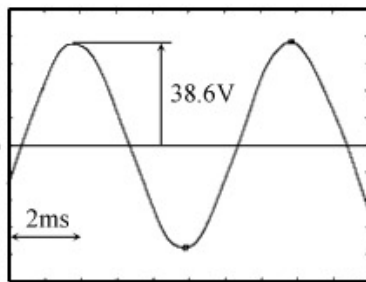
Table 2 Evaluations of resistance and inductance

	Resistance	$L_d$	$L_q$
Measured	$1.39\Omega$	25.0mH	25.0mH
Analyzed	$1.33\Omega$	22.5mH	22.5mH



Inner, Phase

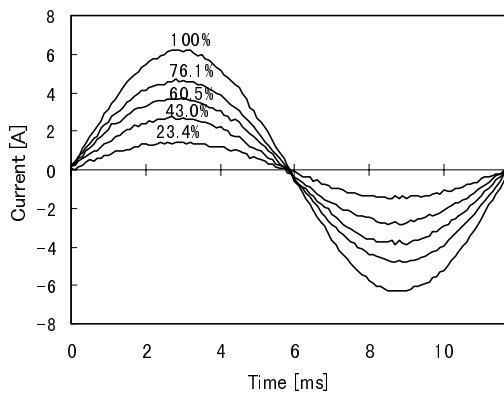
(a) Inner stator



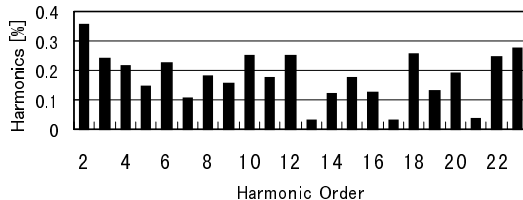
Outer, Phase

(b) Outer stator

Fig. 7 No-load phase voltage at 300r/min.



(a) Current waveforms of various values of load



(b) Frequency spectrum of 100% current

Fig. 8 Current waveforms and frequency spectrum

### 3.3 Voltage and current waveforms

Fig. 7 shows the no-load phase voltage waveforms

with the inner and the outer stators. Table 3 is the summary of the measurements with the voltages. The measured rms value of the voltage is about 8% higher than the analytical value, and the total harmonic distortion is less than 1% with each stator. The results are regarded to be satisfactory.

Table 3 Evaluation of the no-load phase voltage

	rms value	Total Harmonic Distortion
Measured	43.1V	less than 1%
Analyzed	39.9V	--

Fig. 8 shows the current waveforms with various values of load in Test B and the frequency spectrum of the 100% current. As to be seen, the waveforms are almost sinusoidal and all the harmonic components are less than 0.4% in the rated current.

From the above results, it is confirmed the harmonic components in the induced voltage and the current distortion due to the armature reactance are negligible.

### 3.4 Torque characteristics and power flow

Fig. 9 indicates the measured characteristics of the torque versus the current in Test A at 100, 200, and 300r/min. On the graph the ideal characteristics is also plotted, which is calculated from the following equation.

$$T = 3EI/\omega_m \quad (2)$$

where  $E$  and  $I$  are the effective values of the fundamental components of the no-load induced phase voltage and the input current, respectively, and  $\omega_m$  [rad/s] is the angular rotational speed of the rotor.

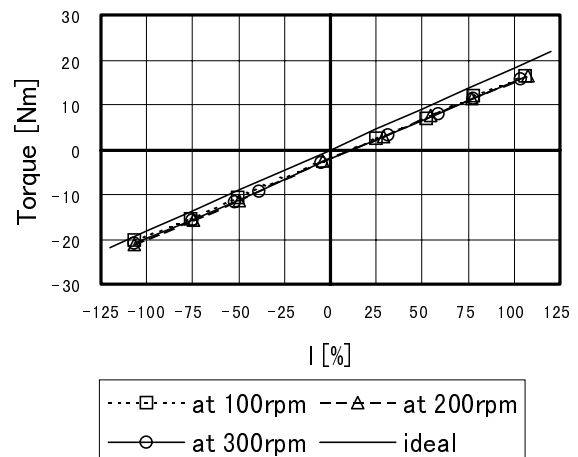


Fig. 9 Torque vs. Current characteristics

It is noticeable in Fig. 9 that there is a relatively large discrepancy between the measured torque and the ideal

one. This is due to two factors; one is the mechanical loss, and the other is a part of the iron losses. In the two factors, the mechanical loss is considered to be dominant, because of the usage of the high friction ring-shaped bearing as mentioned in Section 2. Hence, by replacing it with a low friction type, the mechanical loss will be reduced significantly.

Due to this torque decrease, the rated torque of the motor operation becomes 15.1 Nm, which is about 11% lower than the designed value. Nevertheless, the rated torque of the prototype is about 1.5 times higher than that of the conventional permanent magnet machines, in which the rated torque is as large as 10 Nm.

It is also noted in Fig. 9 that the dependency of the characteristics on the rotational speed is small.

Fig. 10 indicates the power flow of the prototype at 300r/min. The power was measured with Test B because it is generally more accurate to measure the electric power of a motor operating as a generator with linear load than in the case the motor is driven by an inverter. For this reason, both values of the current and the power in Fig. 10 are negative. The shaft power is separated into the effective power, the copper loss, and the iron and mechanical losses.

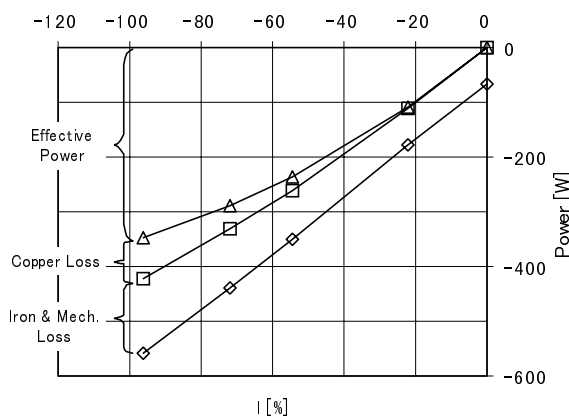


Fig. 10 Power flow of the prototype at 300r/min.

The most obvious fact here is that the iron and mechanical losses are quite large, which corresponds to 24% of the total power. From the fact that the shaft torque is 2.2Nm at no load and 19.3Nm with 100% current, and that the mechanical loss is constant at the same speed, the maximum possible value of the mechanical loss is about  $(2.2/19.3=)$  11%, which implies that there is at least  $(24-11=)$  13% of the iron losses. This is much higher than the common value of the iron losses, which is about 2–5% in the conventional permanent magnet machines. The reason is considered

to be that the prototype has a few factors to increase the iron losses, such as the short circuit of the edges of the steel laminations and the deterioration of the material properties, due to the filing of the tooth-tips of the stators and the rotor yoke surface to adjust the dimensions.

Fig. 11 shows the torque vs. current characteristics in Test A and Test B, both at 300 r/min. It can be confirmed that the two curves are almost identical.

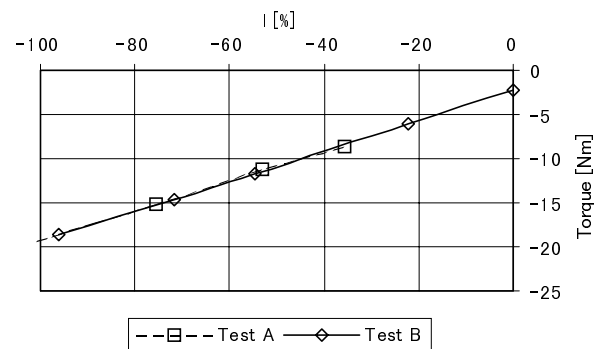


Fig. 11 Torque vs. current characteristics in Test A and Test B (300/min)

### 3.5 Cogging Torque and Torque ripple

To observe the cogging torque, the shaft torque of the prototype was measured at 1r/min with opening the coil terminals. However, the torque component corresponding to the order of the cogging was not observed.

Fig. 12 shows the torque of the machine at 10r/min when the terminals are short-circuited. The major torque fluctuation is the one oscillating once in a rotor rotation, which is not because of the space harmonics of the airgap magnetic field but because of the eccentricity. Therefore, the torque of the DEPMVM is confirmed to be significantly smooth.

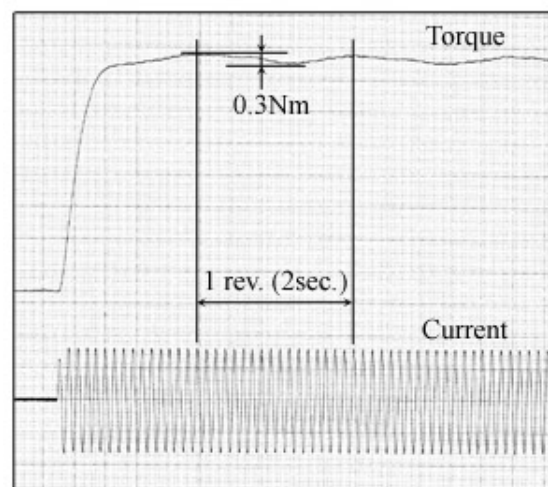


Fig. 12 Shaft torque of the prototype with short-circuited coils (10r/min.)

## 4 Conclusions

The experimental evaluations of the DEPMVM have been presented. The major confirmed items are as follows:

- The rated torque of the prototype is 15.1Nm, which is about 11% lower than the designed value. This discrepancy is mainly due to the mechanical loss. This rated torque, with 130mm of diameter and 60mm of axial length, is more than 1.5 times larger than that of the usual permanent magnet motor of the same size.
- The iron losses have been revealed to be too high, which is at least 13% of the shaft torque at the rated operation. This is considered to be because of the deterioration of the magnetic property with parts of the prototype machine due to its fabrication processes.
- The torque becomes remarkably smooth.
- The measured resistance, inductance, and no-load induced voltage have agreed well with the analysis.

## References

- [1] F.Libbre and D.Matt, "High Performance Vernier Reluctance Magnet Machine. Application to Electric Vehicle," Proc. of EPE '95, pp.2.889-2.894.
  - [2] A.Ishizaki, T.Tanaka, K.Takasaki, and S.Nishikata, "Theory and Optimum Design of PM Vernier Motor," Proceedings of IEE ICEMD '95, pp.208-212.
  - [3] B.C.Mecrow and A.G.Jack, "A New High Torque Density Permanent Magnet Machine Configuration," Proceedings of ICEM '90, pp.1046-1052.
  - [4] A.Toba and T.A.Lipo, "Generic Torque-Maximizing Design Methodology of Permanent Magnet Vernier Machine," Proceedings of IEEE-IEMDC '99, pp.522-524.
  - [5] A. Toba and T.A. Lipo, "Novel Dual-Excitation Permanent Magnet Vernier Machine," Conference Record of IEEE-IAS Annual Meeting '99, pp.2539-2544.
-